CrossMark

An integrated study on the characterization of freshwater lens in a coastal aquifer of Southern India

S. Sathish [1,2] · L. Elango [1]

Abstract The hydrogeochemical characterization of groundwater helps to assess the trend of salinization and freshening of the groundwater. The present study was carried out to understand the lateral and vertical variation of groundwater salinity and the process of salinization and freshening of the groundwater in a coastal aquifer comprising a freshwater lens. The partially isolated unconfined aquifer selected for the present study is lying just south of the Chennai City, one of the densely populated cities on the east coast of South India. Critical problems affecting this aquifer include a thin aquifer which is connected/surrounded by saltwater on all the sides, overexploitation of the groundwater, surface impermeabilization due to increasing residential areas, and destruction of existing dune morphology by conversion of barren land to the residential area which causes a reduction in their barrier effect to seawater intrusion. The process of salinization and freshening of the groundwater was studied and monitored by using electrical resistivity survey and hydrogeochemical analysis. The vertical electrical sounding was carried out at 17 locations, and 400 water samples were collected and analyzed from 50 locations during the period from August 2008 to May 2010 for this study. The apparent resistivity values were analyzed and compared with groundwater quality to demarcate the zone of seawater intrusion. The regional flow direction of the groundwater is westward and eastward with respect to the central stretch and groundwater level ranges from 4.96 m MSL at the dune morphology to 0 m MSL along the boundary on all the sides. Base exchange index indicates that salinization trend in the northern part of the study area is due to the extensive groundwater pumping which increases the possibility of seawater intrusion. The increase of base exchange index towards southern part indicates a better groundwater quality of the aquifer due to proper land use practices. A strong trend of quality alteration is clearly visible from the base exchange index in response to the seasonal change between monsoon and dry season. In the western side, the monsoonal variation in the salinization and freshening of the groundwater was not noticed; however, the salinity is slightly higher than freshwater due to the presence of clay.

Keywords Seawater intrusion · Vertical electrical sounding · Salinity · Base exchange reaction · Freshwater lens · Hydrogeochemical analysis

✉ L. Elango
elango@annauniv.edu

S. Sathish
s.sathish.au@gmail.com

1 Department of Geology, Anna University, Chennai, Tamil Nadu 600025, India

2 Present address: Department of Geology, Adigrat University, Adigrat, Ethiopia

Introduction

Groundwater occurring in coastal aquifers is highly vulnerable to contamination due to over use. The quality of groundwater in shallow aquifer is severely affected by human intervention (Hinrichsen 2007). The hydrogeochemical composition of the coastal groundwater is highly vulnerable to seawater intrusion, and the quality must be regularly monitored. Seawater intrusion is a global environmental phenomenon changing the chemical composition of the coastal groundwater and probably going to worsen in the future as a result of sea level rise associated with climate change (Antonellini et al. 2008; IPCC 2007). The dominant rate of

groundwater pumping than the rate of recharge will reduce the availability of freshwater in the coastal aquifer. Also, the salinity in the coastal groundwater can be induced by marine transgression (Kooi et al. 2000), sea spray spreading (Smith and Johnson 2011), upcoming of connate saline water (Gondwe 1990), and seawater flooding (Apello and Willemsen 1987). The lateral and vertical gradation in the groundwater salinity occurs due to the migration of seawater into the coastal aquifer to maintain density equilibrium. The influence of seawater and the range of salinizations changes from place to place depend on the aquifer characteristics, land use practice, and recharge and discharge of the groundwater. Hence, it is very important to understand the process of salinization to manage the freshwater availability in the coastal aquifer for various usages.

The 7500-km stretched Indian coastline is inhabited by 25 % of the total Indian population (CRZ 2010), and the coastal aquifers are severely affected by the seawater intrusion. Most of these areas are coming under the vulnerable zones because of the increased population density and industrialization which demands more groundwater pumping. Previously in December 2004, the coastal aquifers along the south-east of India were affected by tsunami and the increased chloride concentration comes under normal value after 3 years of rainfall recharge (Sivakumar and Elango 2010). The coastal aquifer located at south of Chennai, India is subjected to seawater intrusion since several decades (Elango et al. 1992; Gnanasundar and Elango 1998, 1999, 2000), and several policies were made to reduce groundwater pumping which is mentioned in "The Chennai Metropolitan Area Groundwater (Regulation) Act 27" (1987). Research works have been carried out by many researchers like Elango et al. (1992), Gnanasundar and Elango (1998, 1999, 2000), Sathish et al. (2011), and Sathish and Elango (2015) to analyze the status of seawater intrusion in the area of study by using electrical resistivity survey, major ion characterization, and by development of numerical model. The problems occurring in this coastal unconfined aquifer include the presence of saltwater on all the sides, overexploitation of groundwater, lack of natural recharge due to land impermeabilization as a result of urbanization and settlements, destruction of natural beach dunes leading to the reduction of their barrier effect to seawater intrusion, and improper drainage system. All these factors promote seawater intrusion into this coastal freshwater aquifer, and still this aquifer is being used for the supply of groundwater to the Chennai City needs. The surface water with high concentration of salt at all the sides causing a density gradient towards the freshwater aquifer at various distances depends on the rate of pumping of groundwater (Sathish and Elango 2011). The density gradient in coastal groundwater is due to the difference in density between freshwater and seawater, and

the lower density freshwater lens overlie the higher density saltwater wedge (Bear et al. 1999; Post and Simmons 2005; Bereslavskii 2006; Mollema et al. 2010). An understanding of changes in the freshwater lens that overlie saltwater wedge from all the sides will be useful to manage groundwater resources in the south Chennai coastal aquifer. Hence, in addition to previous research work carried out by several authors in this area, the present study was carried out with the objective to understand the lateral and vertical variation of groundwater salinity and variation in the process of salinization and freshening of groundwater under various seasons. The salinization and cation exchange process are fortunately happening when the groundwater is mixing with seawater (Stuyfzand 2008; Kouzana et al. 2010). The approaches to study this particular problem have been managed by using electrical resistivity understanding of the aquifer, measurement of salinity, and calculation of cation exchange behavior of the groundwater with seawater (Massoud et al. 2015; Gimenez forcoda 2010). The change in the salinity and freshness of groundwater was mainly triggered by the heavy groundwater pumping that will induce the mixing of saltwater with freshwater in this aquifer. Irrigation in this area is minimal; hence, the salinity due to irrigation is not considered in this work.

Study area

The study area is located on the east coast of south India and lies south of Chennai metropolitan city. The area is surrounded by the Bay of Bengal in the east, Buckingham canal in the west, and the Adyar River and Muttukadu backwaters in the north and south, respectively (Fig. 1). The topographical elevation ranges from sea level to maximum elevation of 12 m MSL (Fig. 2a). The Precambrian gneiss of charnockitic composition is the basement rock of the study area. The weathered charnockitic rock of variable thickness is overlaid by unconsolidated quaternary sediments with a thickness ranging between 10 and 24 m. The quaternary sediments comprised of sand, clay, sandy clay, and clayey sand. The sandy formation covers most part of the area, and the clay, sandy clay, and clayey sand are present as patches in between the sand formation. Along the western boundary, i.e., along the Buckingham canal, clay is the dominant formation. The upper unconsolidated formation and lower weathered formations function as an unconfined aquifer.

The southwest monsoon prevails from July to September, and the northeast monsoon is active from October to December. The remaining months from January to May are considered as a transition or dry period. The annual average rainfall is about 1200 mm. Temperature varies in summer between 35 and 42 °C, and in winter it ranges from 25 to 34 °C. The geomorphologic features present in the area are sand dunes, beach, and

Fig. 1 Location of the study area
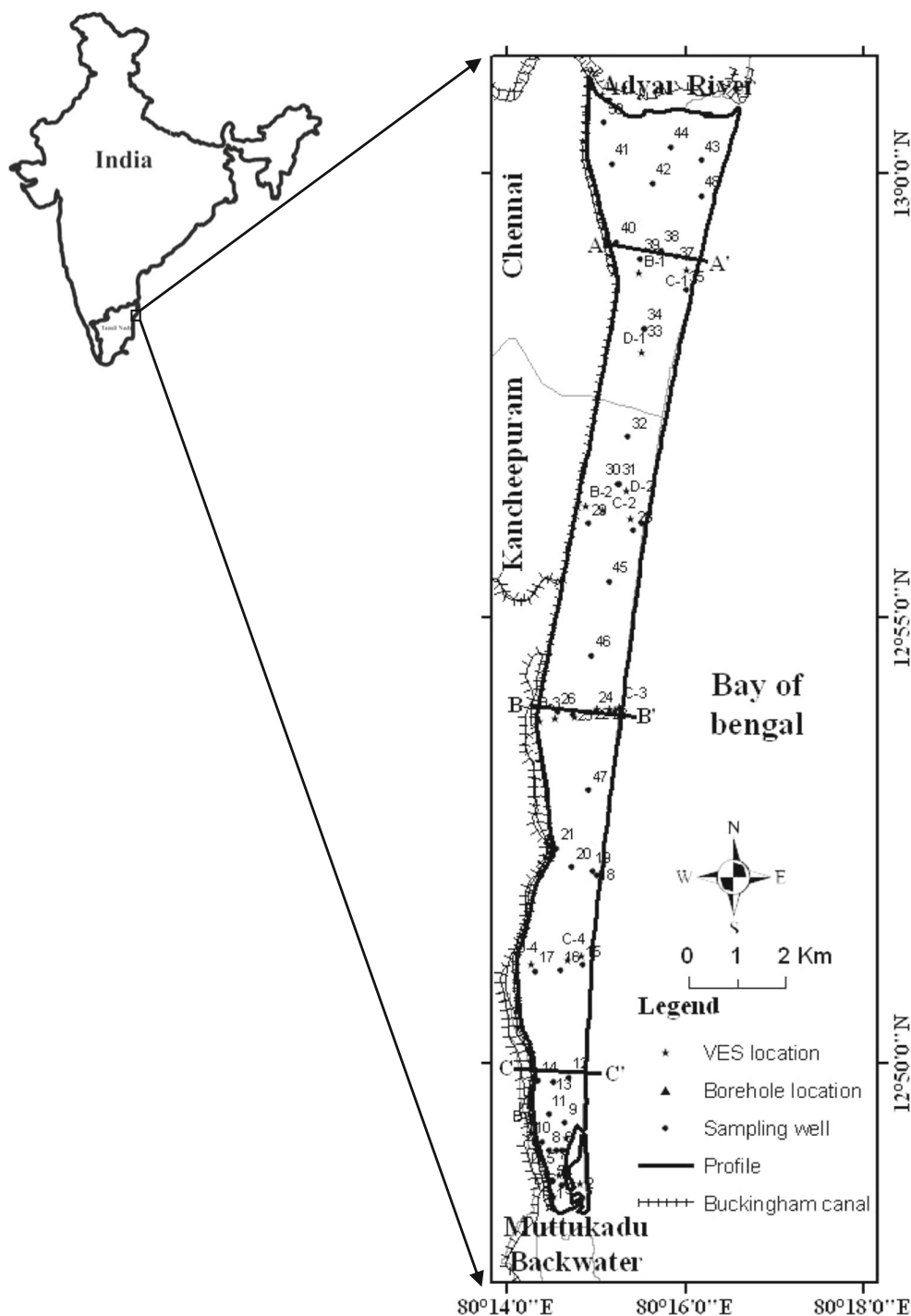
terraces. The land use and land cover pattern are primarily composed of urban settlements, aquaculture, recreational theme parks, and hotels and secondarily by agricultural land and small-scale industries. The urbanization is comparatively large in the northern part (Fig. 2b). The groundwater flow in this region follows the hydraulic head difference resulting from topographic relief (Gnanasundar and Elango 2000). However, short-term variation in the groundwater flow that allows lateral and vertical mixing

of groundwater occurs due to heavy pumping. Gnanasundar and Elango (2000) reported that the excessive groundwater withdrawal in this area causes seawater intrusion. Kuzhali et al. (2009) stated that before 1950s this area was undisturbed by means of human activities, and from 1950s to 1985, industrialization and settlements developed from the northern part of the study area. In the period from 1985 to 1997, there was a steep increase in settlements which induced the seawater intrusion due to

Fig. 2 a Topography of the area. **b** Land use and land cover map derived from IRS-LISS III (February 2004)
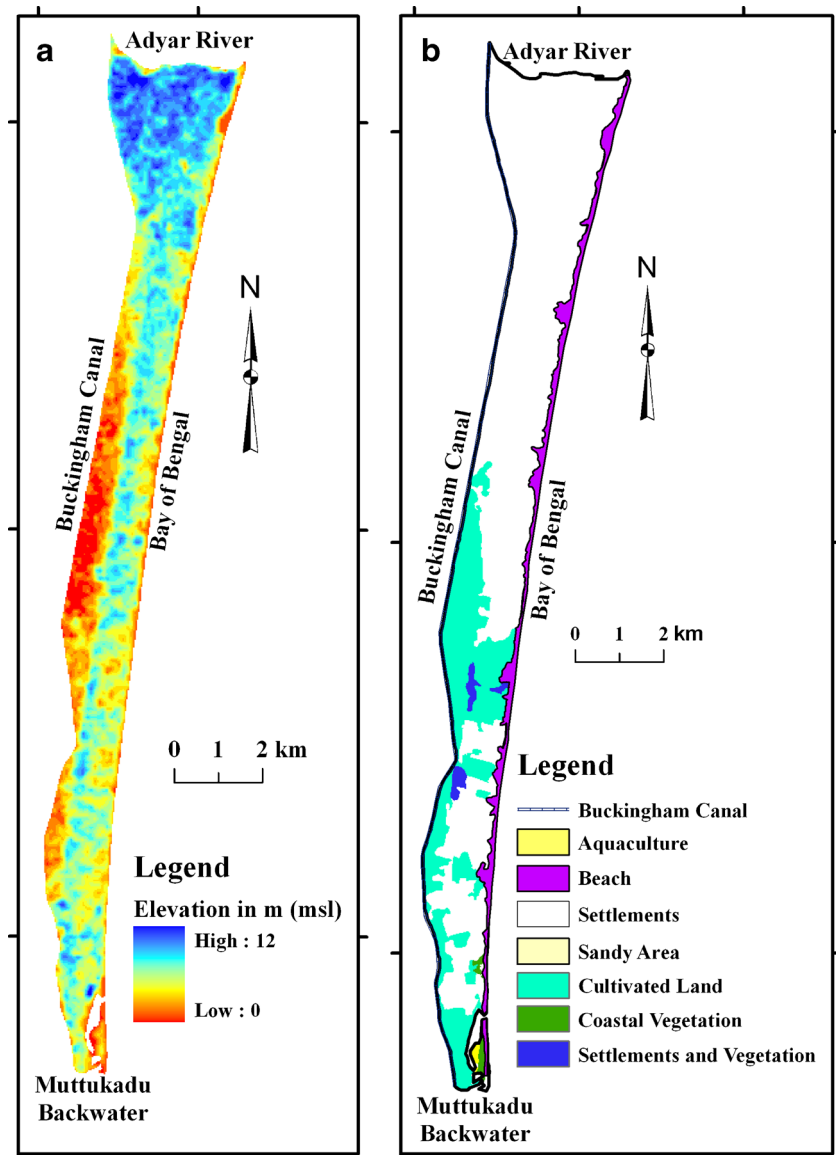
heavy groundwater pumping from this thin freshwater aquifer. From 1997 to 2006, there was a rapid growth of many industries at various scales following the economic boom and unluckily this leads to a deterioration of the environment and its natural resources. In 2002, there was a government act that made rainwater harvesting mandatory in all buildings to avoid seawater intrusion by means of increasing groundwater recharge. This aquifer is one of the major sources of groundwater to the public and industrial activities with a withdrawal of groundwater varying between 0.131 and 0.199 m^3 day^{-1} in 2010 (Senthil et al. 2001; Sathish and Elango 2015). The pumping of groundwater by government well fields was reduced than earlier, but still the private houses located in this region also have wells to meet their needs. In the present situation, the environmental and ecological imbalance is arising in the coastal area due to overexploitation of groundwater

because of increase in settlements, hotels, tourism centers, and many industrial activities that are also affecting the availability of freshwater in this relevant aquifer.

Material and methodology

From the literature, it is clearly understood that this aquifer is affected by seawater intrusion for a prolonged time. Electrical resistivity survey is an excellent tool to delineate the boundary between seawater and freshwater (Barker 1980; Griffith and Barker 1993). Additionally, it will provide information relatively to the depth of the saturated medium (Sathish et al. 2011; De Franco et al. 2009; Adepelumi et al. 2009; Lee and Song 2007b; Nowroozi et al. 1999; Goldman et al. 1991). After starting electrical prospecting for earth's material by Robert W. Fox in 1830s for making use of natural current,

many researchers were focused on electrical prospecting that was initially for ore bodies. Usage of direct or low-frequency alternating current to detect the subsurface begins with Schlumberger and Wenner in the beginning of 1900s. Later on, electrical resistivity survey has been used for aquifer characterization from 1930s (Sundberg 1932; Senthil kumar et al. 2001; Shevnin et al. 2006) like groundwater quality assessment (Corriols and Dahlin 2008; Park et al. 2007; Lee and Song 2006), zone of liquefaction (Balkaya et al. 2009) and identification of features like sinkholes (Garman and Purcell 2004), fractures (Yadav and Singh 2007), etc. Basically in the subsurface, current flow is formed in two ways that include electronic and electrolytic conduction (Zhang et al. 1995; Keller and Freschknecht 1966). The aquifer is composed of sand which is a mixture of quartz and feldspar. Hence, the flow of current is dominated by an electrolytic solution which is groundwater that is available in the porous medium of the saturated formation. In the unsaturated medium, role of metallic ions in feldspar, partially filled groundwater in the porous medium, and moisture content plays a major role for current flow. In the unsaturated clay, the conduction is motivated by metallic ions (Worthington 1993; Oskay et al. 1993; Kelly 1977; Waxman and Smith 1968; Archie 1942; Sundberg 1932). Due to variation in density and concentration of electrolyte (groundwater), the contrast between seawater and freshwater is easily understandable by qualitative and quantitative interpretation of electrical resistivity data (Sathish et al. 2011; Kouzana et al. 2010; Adepelumi et al. 2009; Benkabbour et al. 2004). Hence, the electrical resistivity surveys have been employed to delineate the zone of seawater intrusion in the current study.

The electrical resistivity survey was conducted by using Vertical Electrical Sounding (VES) method. The locations were marked along the coastal zone, canal boundary, and the dune geomorphic features in such a way to identify groundwater flow and lateral and vertical changes in the quality of groundwater. Care was taken for the site selection to avoid failure in resistivity measurements by means of surface inhomogeneity, the presence of buried conductors, etc. (Stollar and Roux 1975). Totally 17 locations were chosen to cover the entire area of around 23 km length and width of 1 to 3 km. The accuracy of the result mainly depends on the type of array, spacing between electrodes, type of formation present beneath the subsurface, measurability of the signal by the equipment, and ability to reduce the noise (Bernard 2003; Srinivasa Gowd 2004). The Schlumberger (1920) array has been employed by using Terrameter SAS 1000/4000 which is one of the best and widely used array for delineating the seawater and freshwater interface (Nowroozi et al. 1999). The maximum spacing between current electrodes was 160 m. To avoid ambiguity in the results due to less apparent resistivity obtained for both clay and seawater intruded zone, the quantitative interpretation was made by comparing borehole logs available in the

nearby location. The quantitative measure of thickness and apparent resistivity of the each electrical resistivity layer was measured by forward modeling (Davis et al. 1980; Anderson 1989) by introducing the known lithological layers. The inversion of nonlinear measured field data was done by ridge regression analysis (Inman 1975) which is a standard technique for correlation (Jupp and Vozoff 1975). The multiple iteration curve matching technique was adopted without disturbing the measured field data by using Resist IX1D software. The layer model and smooth model curve were obtained, and the parameters such as the thickness of unsaturated zone, saturated zone, the thickness of lithological layers, and apparent resistivity of each layer were finalized. The low resistivity zone representing a zone of seawater intrusion was identified. Electrical resistivity methods can be used to identify the contaminated zone, but still, it cannot be able to give information about the chemical characteristics of the aquifer. Hence, an integrated study of electrical resistivity and geochemical analysis will reduce the limitations of both methods and will give a better understanding of the aquifer (Sonkamble 2014). In addition to the electric resistivity methods, groundwater monitoring, hydrogeochemical analysis, and hydrogeochemical indicators were used to characterize the groundwater quality and process of salinization and freshening of groundwater within the coastal aquifer.

The groundwater monitoring was started in August 2008 in various large diameter wells and bore wells located in the study area. Since then, all the wells were periodically monitored at 3-month interval until May 2010. Totally 50 samples were collected during each monitoring period. It includes 49 well samples and 1 surface water sample from the canal. About 500 ml of sample was collected in a clean polyethylene bottle from each location. The collected samples were subjected to physical and chemical characteristics analysis. In total, 87.8 % of the monitored wells are less than 10 m in depth and the depth of the well varies from 3 to 18.4 m. The groundwater level, electrical conductivity (EC, $\mu S\ cm^{-1}$) and temperature (T, °C) were measured in the field by using portable meters. The samples were preserved at the Department of Geology, Anna University, Chennai until the determination of the concentration of various parameters by titration and ion chromatograph (Metrohm). During the month of May 2010, the vertical variations of EC and T were measured in all the bore wells until the depth of 0.5 m above the bottom. The data were organized in profiles passing through the well locations normal to the coast from the sea to the Buckingham canal (Fig. 1). Three profiles were created to calculate the thickness of freshwater availability.

The boundary of freshwater lens is defined by using the salinity standard for drinking purpose that is less than or equal to 1 g l^{-1}. Several algorithms are available to calculate salinity such as by using ratio of mass of

seawater (Knudsen 1901), EC and chlorinity relationship (Cox et al. 1967), conductivity and mass of seawater relationship (UNESCO 1981a), etc. The algorithm based on practical salinity scale (PSS), which is the function of EC, temperature, and pressure published by UNESCO (1983), was used to calculate the salinity. This algorithm gives promising accuracy in between calculated and field salinity of water samples having temperature ranges between −2 and 40 °C. By using the developed algorithm given by Eq. (1), the variations of salinity across lateral and vertical directions were calculated by using EC and temperature that was measured from the field. In order to create a 2D section of salinity variation, the salinity measured from the canal and the salinity of 31.06 g l^{-1} (Mondal et al. 2011) for the Bay of Bengal were also used together with the salinity values obtained from the wells. The section (one for each profile) has been created by using Rockworks 2006 and Arc GIS 9.1.

$$\text{Salinity}\left(gl^{-1}\right) = a_0 + a_1 R_t^{1/2} + a_2 R_t + a_3 R_t^{3/2} + a_4 R_t^2 + a_5 R_t^{5/2} + \Delta S \tag{1}$$

where a, R_t, and ΔS are constants that will vary based on three factors such as EC ($\mu S\ cm^{-1}$), $T\ °C$, and pressure measured in the field.

The base exchange was first recognized by Versluys during the period of 1916 (Stuyfzand 2008) who used equivalence of sodium, calcium, and magnesium. Many theories behind the chemical concentrations of water were started from Arrhenius in 1887, and the increase in the concentration of ions will increase the activity of ionic exchange as a function of pressure and temperature (Fetter 2001). Hence, the hydrogeochemical modification of groundwater by seawater intrusion has been attributed to base exchange reactions as given in Eq. 2 (Vengosh 2003). The freshwater is dominated by the Ca^{2+}–HCO_3^- equilibrium, whereas the seawater is dominated by the Na^+–Cl^- equilibrium. During the mixing of high concentrated seawater with low concentrated groundwater, at the high activity, monovalent cation Na^+ replaces divalent cations such as Ca^{2+} and Mg^{2+}. The reversible reaction can also be possible when Ca^{2+}- and Mg^{2+}-enriched clays are present. The presence of shells in the aquifer also contributes to reversible reaction due to the presence of calcium in its composition (Fetter 2001). In the case of the anion, HCO_3^- is replaced by Cl^-.

$$Na^+ + \frac{1}{2}Ca–X_2 \leftrightarrow Na–X + \frac{1}{2}Ca^{2+} \tag{2}$$
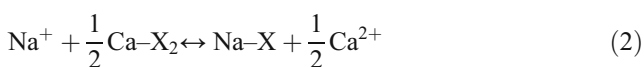
The base exchange index (BEX) is a molar ratio that indicates salinization and freshening of the groundwater. The process of base exchange is also attributed by minerals present in the aquifer. One of the mostly used hydrogeochemical index among the all those available (Table 1) is that of Stuyfzand (1986). This BEX formula

Table 1 Overview of BEX formula from literature (Stuyfzand 2008)

No.	Author	Index (meq/l)
1	Versluys (1916, 1931)	$Na^+/(Na^+ + Ca^{2+} + Mg^{2+})$
2	Schoeller (1934)	$(Cl^- – (Na^+ + K^+))/Cl^-$
3	Schoeller (1956)	$(Na^+ + K^+)/Cl^-$
4	Schoeller (1956)	$(Ca^{2+} + Mg^{2+})/(HCO_3^- + CO_3^{2-} + SO_4^{2-})$
5	Delecourt (1941)	$Na^+ + K^+ – Cl^-$
6	Stuyfzand (1986)[a]	$Na^+ + K^+ + Mg^{2+} – 1.0716\ Cl^-$
7	Stuyfzand (2008)	$Na^+ + K^+ – 0.8768\ Cl^-$

[a] Used in this study

proposed by Stuyfzand (1986) is suitable for this study area because the aquifer mainly consists of quartz and feldspar with nil carbonate (Gnanasundar and Elango 1998). Integer negative BEX indicates salinization of the groundwater, and integer positive BEX indicates freshening of the groundwater. The zero indicates a conservative equilibrium state between seawater and freshwater.

Results and discussion

Vertical electrical sounding

The coastal zone and dune surface are mostly covered with sand. The type of curve is QHA with five number of electrical resistivity layers ($\rho_1 > \rho_2 > \rho_3 < \rho_4 < \rho_5$). The top electrical resistivity layer always represents the unsaturated formation of varying thickness from place to place. It is followed by saturated sand, a mixture of sand and clay, weathered zone, and basement rock. The locations D5 and C6 in the south end represent four electrical resistivity layers, and a layer comprising a mixture of sand and clay is absent with type curve HA ($\rho_1 > \rho_2 < \rho_3 < \rho_4$). It is also confirmed with nearby borehole lithologs (Fig. 3).

The first layer comprised of unsaturated sand with the thickness ranges from 1.3 m in the location C-4 to 7 m in the location D-5 and the apparent resistivity ranges from 249.9 to 17,881.1 Ω-m. The second layer consisting of saturated sand with the thickness varies from 1.2 m in the location C-2 to 10.3 m in the location C-6. The apparent resistivity value ranges from 3.2 to 826.8 Ω-m (Table 2). The apparent resistivity value between 3.2 and 45.1 Ω-m indicates the influence of seawater which is noticed in all the locations except C2 and C5. The freshwater layer usually floats on the high-density saline water along the coastal boundary which is not identified due to its insignificant thickness (Hodlur et al. 2010). In the locations C-2 and C-5, the influence of seawater is not identified in the entire saturated layer. In the C-2 location, the thickness of the aquifer is shallow and depth to hard rock is lesser than

Fig. 3 Inversion of field data and comparison of lithologies from borehole stratigraphy
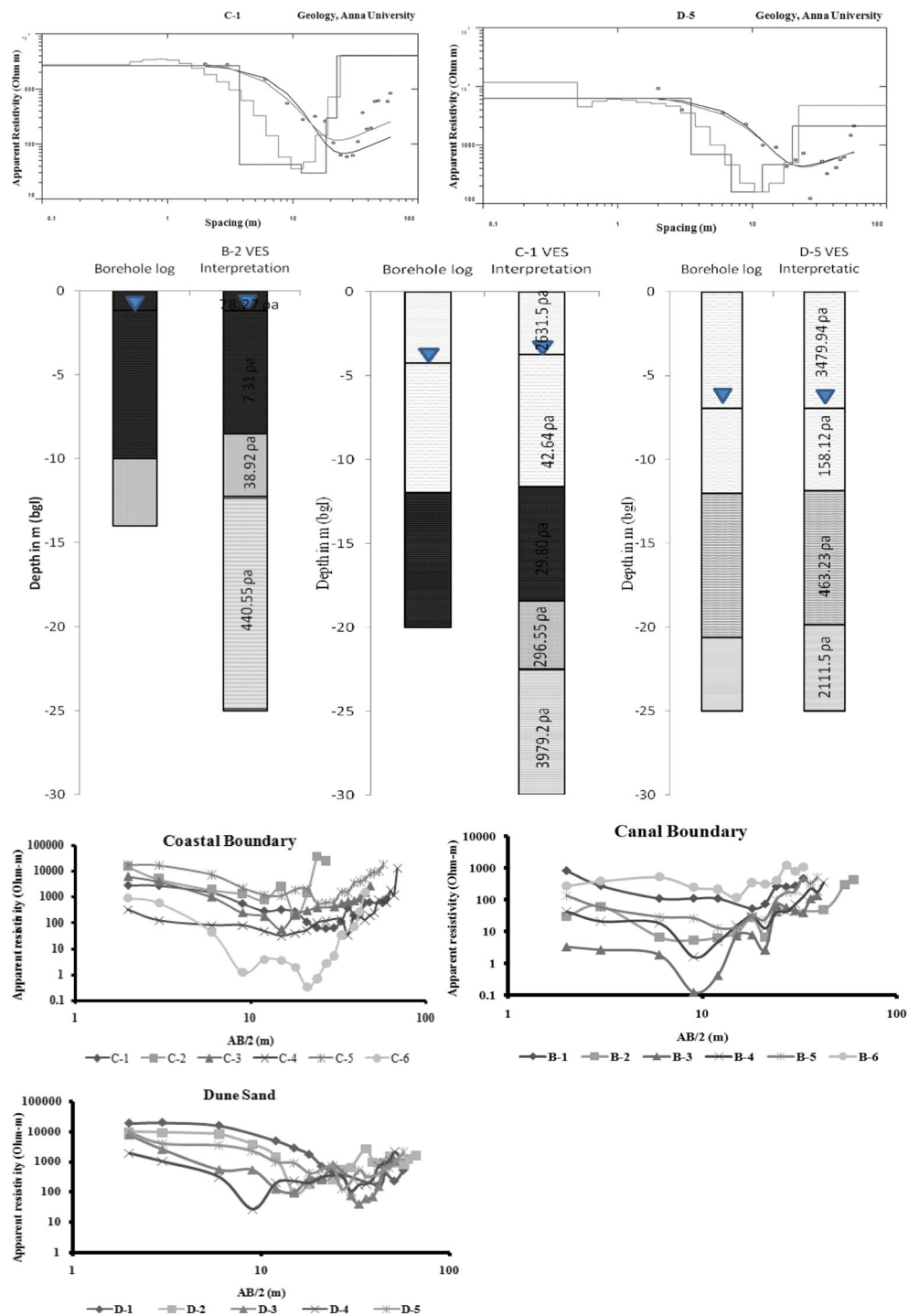
the remaining locations in the coastal zone, whereas in the location C-5, the thickness of freshwater is expected to be high with the absence of seawater intrusion.

The third layer is made up of a mixture of sand and clay with thickness ranging from 1.3 to 6.9 m in the C-2 and C-3 locations, respectively. The apparent resistivity is also less in this layer along the coastal zone like in the first layer. The thickness is less in the central part at the dune surface, reaching high thickness on both sides towards the canal, and

the sea subsequently acquires a concave shape to the layer. In the dune surface, this layer has a thickness of 1.1 m in the location D-4 to 4.7 m in the location D-3. In the western side, it is connected with the outcropped clay and sandy clay along the boundary of the canal. The lesser apparent resistivity value along the coastal boundary varies from 1.1 to 33.8 Ω-m due to high conductance caused by seawater intrusion and may also due to the process of cation exchange which is usually high in the clay minerals as mentioned by Shevnin et al. (2007).

Table 2 Results of curve matching by inversion of field data

Location	Unsaturated		Saturated							
	Thickness of layer I (sand) in m	ρ_a in Ω-m	Thickness of layer II (sand) in m	ρ_a in Ω-m	Thickness of layer III (clay/sandy clay) in m	ρ_a in Ω-m	Thickness of layer IV (weathered charnockite) in m	ρ_a in Ω-m	Thickness of layer V (hard rock) in m	ρ_a in Ω-m
Coastal boundary										
C-1	3.6	2538.2	7.3	42.6	6.5	33.8	4.5	296.6	∞	3979.2
C-2	3.6	3908.4	1.2	619.4	1.3	120.3	2.0	1308.6	∞	5525.0
C-3	2.0	11,012.1	6.4	11.9	6.9	1.1	7.0	30.6	∞	123.3
C-4	1.3	249.9	8.3	45.1	2.3	16.2	7.0	1674.9	∞	4592.0
C-5	3.3	11,302.4	3.8	826.8	2.7	387.4	7.0	1970.6	∞	5934.7
C-6	2.0	835.2	10.3	3.2	Absent	NA	3.7	20.8	∞	1633.1
Dune surface										
D-1	6.7	17,881.1	5.2	360.4	2.1	104.2	9.7	145.2	∞	2563.3
D-2	5.0	9441.3	2.1	98.1	1.8	77.2	6.7	1363.7	∞	20,130
D-3	3.4	9782.3	3.6	129.8	4.7	86.7	7.6	411.3	∞	676.3
D-4	5.7	1291.5	4.3	71.7	1.1	48.8	9.3	700.8	∞	2272.7
D-5	7.0	3479.9	4.9	158.1	Absent	NA	8.0	463.2	∞	2111.5

Location	Layer I (clay/sandy clay) in m	ρ_a in Ω-m	Layer II (clay/sandy clay) in m	ρ_a in Ω-m	Layer III (weathered charnockite) in m	ρ_a in Ω-m	Layer IV (hard rock) in m	ρ_a in Ω-m
Canal boundary								
B-1	3.4	123.3	4.7	60.2	1.8	147.6	∞	489.6
B-2	1.2	78.3	7.3	7.3	3.7	38.9	∞	440.6
B-3	3.7	3.1	5.5	0.8	2.2	6.3	∞	183.6
B-4	3.2	17.8	3.6	6.2	4.1	82.9	∞	344.4
B-5	3.2	35.1	2.8	15.8	5.2	91.1	∞	517.3
B-6	3.3	371.4	4.2	115.1	4.3	690.9	∞	8729.7

The fourth layer is a weathered zone and has a thickness ranging from 2 to 9.7 m. The grade of weathering played a major role to conduct electrolytic flow in this layer. The different grade of weathering is noticed in various locations by means of a different range of electrical resistivity measurements in the field. The successive increase in the electrical resistivity values from the top surface to the bottom of the weathered zone represents a decrease in the grade of weathering. Similarly, a sudden decrease in the deeper level is an indication of the presence of a fracture or weak zone. Finally, the weathered rock is followed by the basement rock to the depth ranging from 8.1 to 23.7 m.

The VES locations along the canal boundary exhibit a low apparent resistivity due to the presence of clay/sandy clay. The thickness of unsaturated zone ranges from 1.2 to 3.7 m with an apparent resistivity ranges from 3.1 to 371.4 Ω-m. The saturated layer includes sandy clay and weathered charnockite which together varies in thickness from 6.5 to 11 m. The depth to the basement rock varies from 9.9 to 12.2 m. A low apparent resistivity is measured in B-3 as 0.8 Ω-m because this area is dominated by clay compared to all the other locations. Similarly, in the locations B-1 and B-6, the apparent resistivity is higher due to limited clay content.

The results obtained by inversion and curve matching techniques are shown in Table 2. Generally, the apparent resistivity is high on the dune surface all over the study area. The higher apparent resistivity in the dune surface is due to the presence of coarse and dry sand. The order and number of layers are similar in all the locations except the locations nearby the western boundary bordering Buckingham canal. Here, the top layer is composed of clay and sandy clay. The VES locations C-1, C-2, C-3, C-4, C-5, and C-6 are located at a distance of 170, 273, 130, 200, 340, and 111 m from the sea. The influence of seawater is identified in all the locations other than C-2 and C-5. However, the seawater intrusion is significantly noticed in C-1 and C-6 locations. These were correlated and confirmed with hydrogeochemical results which are discussed in the later sections. The zone of seawater influence is characterized by a decrease in the value of apparent resistivity. In the VES location C-1, a sudden decrease of apparent resistivity from several thousands to 42.6 Ω-m is noticed. The area where the VES location C-6 is placed is similar to an elongated or island aquifer which is around 400 m width and 1.5 km length. It is surrounded by seawater and backwater on all the sides that occupy the subsurface aquifer and the freshwater thickness is very less as reported by Bakker (2000) and Oude Essink (2001). Hence, in the VES location C-6, the apparent resistivity value decreases down to 0.34 Ω-m (Fig. 3) which gives an apparent resistivity of the entire layer 3.2 Ω-m as an indication of seawater intrusion.

Groundwater monitoring and hydrogeochemical analysis

Groundwater level fluctuations

The groundwater level ranges from 0 m MSL along the boundary at all the sides to 4.96 m MSL in the dune surface (Fig. 4a). The maximum groundwater level of 4.96 m MSL was observed during the monsoon period and the maximum groundwater level of 2.45 m MSL during the dry period of May 2009. The average annual fluctuation in the groundwater level is 1.36 m, and the maximum fluctuation is 2.74 m in the northern part of the study area. The temperature of groundwater ranges from 34.8 to 27.7 °C. The maximum temperature was recorded during the period of May 2009, and the minimum temperature was recorded during August 2009. The EC ranges from 130 to 5250 μS cm^{-1} during the period of investigation. The maximum EC of 5250 μS cm^{-1} was observed along the coastal boundary of the profile A-A′ in the north during the dry season (Fig. 4b). Towards canal, the maximum EC of 2000 μS cm^{-1} was observed during the same period. At the middle of profile A-A′, the observed EC value of 137 μS cm^{-1} is less than the desirable limit which confirms the presence of the freshwater lens. The well located at the south part where the land is surrounded by seawater and backwater on all the sides shows high EC ranging from 1650 to 13,490 μS cm^{-1} during the period of study. The mentioned high EC variation is observed only in one well which is in the extreme south. The maximum value was measured during the dry period, and the minimum value was measured during the end of monsoon. The EC can be increased along the direction of groundwater flow and also when it reaches close to the pollution source. The rock–water interaction could be the reason for the former statement and the process of dispersion, dissolution, etc. could be the reason for the latter. The cross-sectional comparison of groundwater level and EC gives a better understanding of the influence of saltwater presence on all the sides.

Groundwater chemistry and concentration gradient between sea and canal

An abundance of ions in groundwater samples are in the following order: $Na^+ > Ca^{2+} > Mg^{2+} > K^+ = Cl^- > HCO_3^- > SO_4^{2-}$. The type of groundwater in this area is primarily Na^+-Cl^- and secondarily Ca^{2+}-HCO_3^-. The maximum concentration of Na^+ is 4269 mg l^{-1} during the month of May 2009, and the minimum concentration is 8 mg l^{-1} during the month of November 2008. Generally, K^+ concentration in the groundwater is one tenth to one hundredth of Na^+. The K^+ maximum and minimum concentrations vary between 2 and 61 mg l^{-1}. The maximum concentration was measured during May 2009, and the minimum

Fig. 4 **a** Spatial variation in groundwater level (m MSL). **b** Distance from the sea vs. Groundwater level (m) and EC (μS cm^{-1})
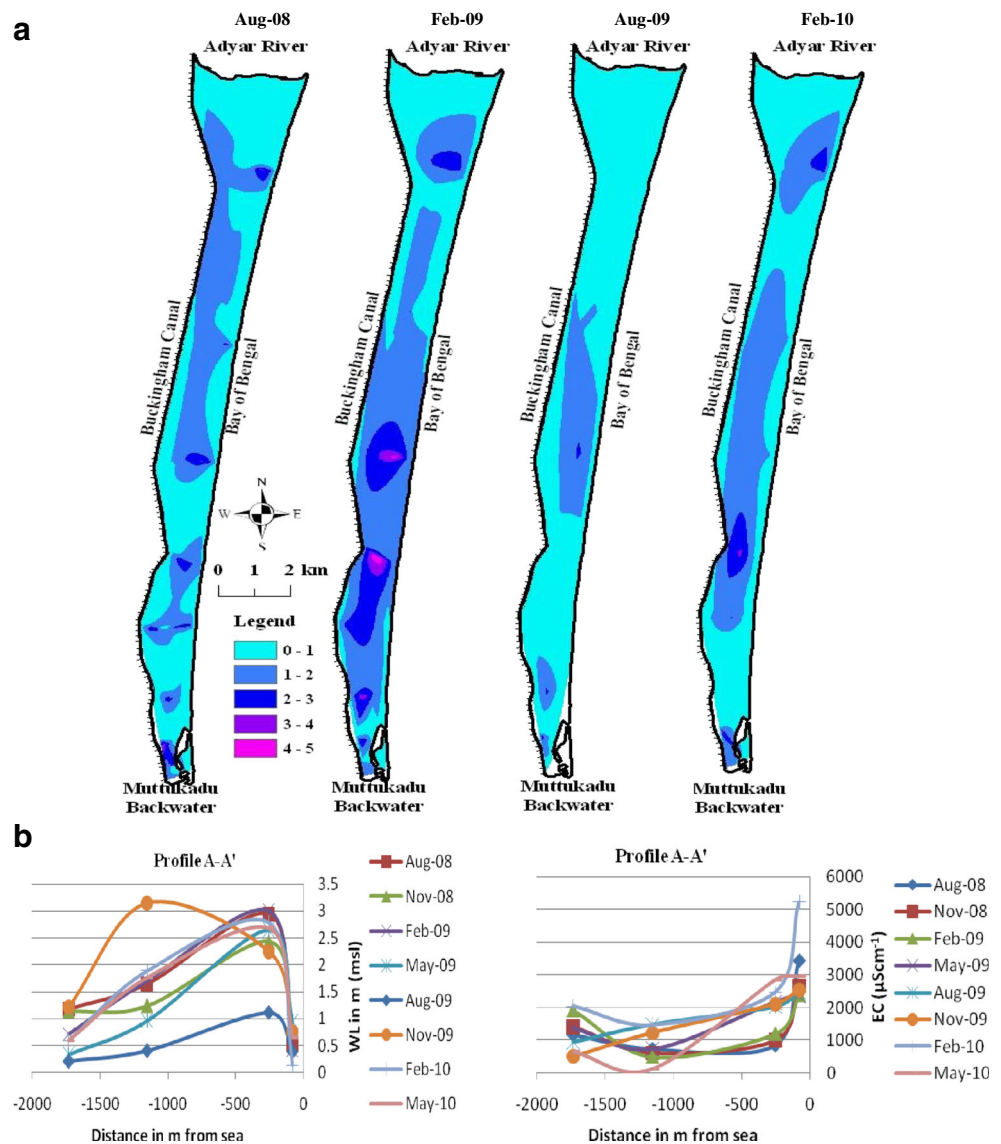
concentration was measured during the monsoon period. The calcium content of the groundwater ranges between 2 and 346 mg l^{-1}. The calcium can be derived from rainfall, aquifer matrix, and shell fragments present in the sandy aquifer. The sandy aquifer also contained shell fragments that dissolve the calcium into the groundwater. The concentration of calcium is inversely proportional to the presence of sodium. The water enriched with sodium may replace calcium in the groundwater and induce the salinity. The concentration of magnesium ranges from 2 to 140 mg l^{-1}. Carbonate is not observed in the groundwater samples collected during the period of study. The concentration of the bicarbonate varies from 21 to 626 mg l^{-1}. The maximum concentration of bicarbonate is recorded during the monsoon period. It is maximum towards the north part and minimum towards the south part of the study area. However, the concentration of bicarbonate is minimum towards the south

still; its contribution to the total concentration of ions in the groundwater is high. Chloride salts, being highly soluble and free from chemical reactions with the minerals present in the aquifer medium, remain stable once they enter into solution. Chloride has a concentration ranging from 10 to 6867 mg l^{-1}. The minimum concentration of chloride was measured in the groundwater samples collected from deep bore wells located in the central part of the study area. The maximum concentration was measured in the well located at the southern most part of the study area during the month of May 2009. The important source for chloride in the study area is the saltwater surrounding the aquifer. Based on the chloride classification proposed by Stuyfzand (1993), the majority of the groundwater samples are primarily of the oligohaline to fresh category in the study area and brackish to saline along the coastal boundaries. The sulfate content in the groundwater varies from 2 to 392 mg l^{-1}.

Salinity

Groundwater salinity calculated from EC, temperature, and pressure measurements ranges from 0.004 to 2.07 g l^{-1} during the monsoon season and from 0.01 to 5.71 g l^{-1} during the dry period as shown in Fig. 5a. The salinity is under the permissible limit (1 g l^{-1}) in the shallow groundwater samples in most of the area. In the area nearby the

mouth of Adyar River in the north and the area bordering Muttukadu backwater in the south represent salinity greater than the permissible limit. The flow of groundwater is a three-dimensional property which follows the gradient of topography as well as the gradient of salinity from low concentration to a higher concentration bordering the study area. A comparative analysis of all the measured and calculated data shows that the interface between seawater

Fig. 5 **a** Variation in salinity (g l^{-1}) during the monsoon and the dry period. **b** Seasonal comparison in rainfall and salinity ranges within the Buckingham Canal
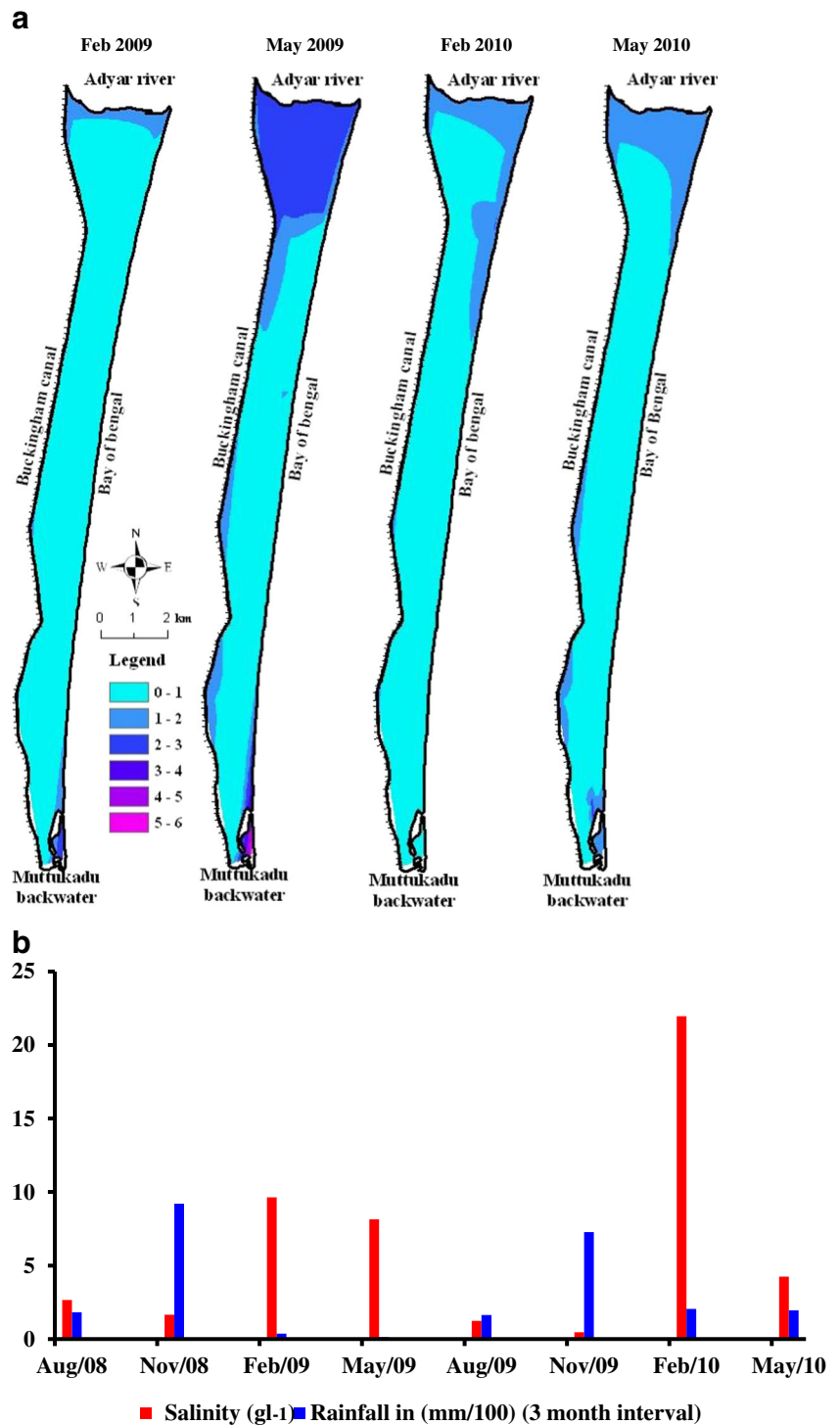
**Fig. 6** Salinity profile between the Buckingham Canal and the sea
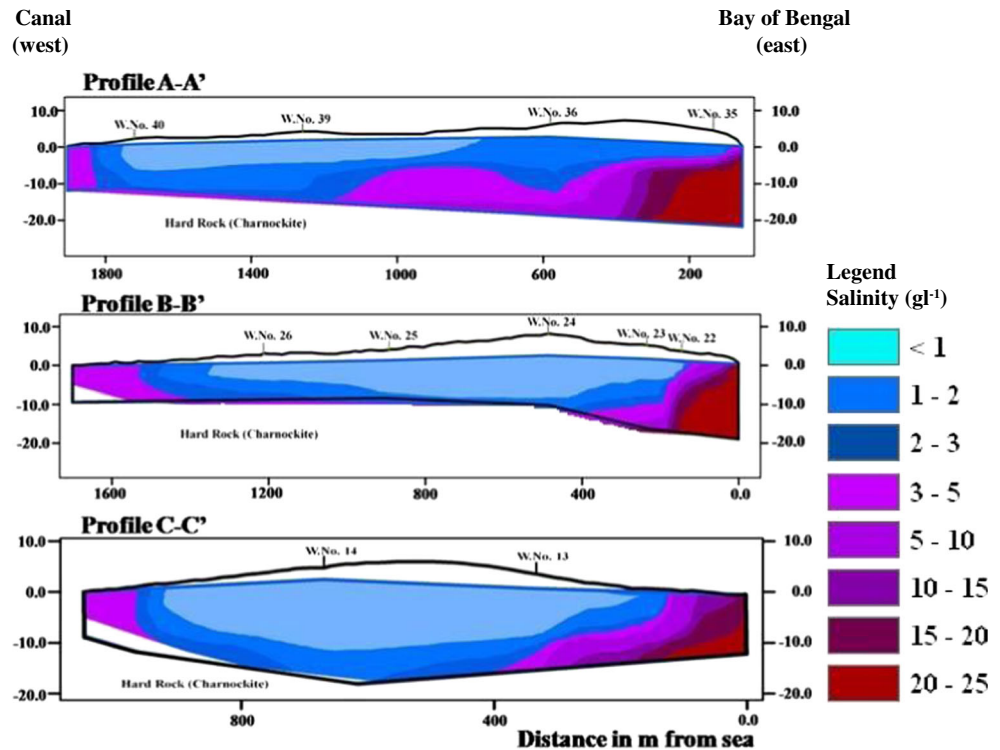
and freshwater is migrating landward during the months of the dry period. This aquifer behaves as a partially isolated aquifer due to the presence of water body on all the sides. The thickness and areal extent of the freshwater lens of the partially elongated aquifer are supposed to be directly proportional to the width of the aquifer as noticed by Bakker (2000) and Oude Essink (2001). In the present study area, the areal extent of freshwater lens is inversely proportional to the width of the aquifer. Towards the northern part, the width of the aquifer is larger but the areal extent of the freshwater lens is smaller than the south. It indicates the heavy pumping of the groundwater that induces intrusion of seawater and subsequent decrease in areal extent of the freshwater lens in the northern part.

The canal contains stagnant brackish water and is connected to the sea by means of Muttukadu backwater in the south and by the Adyar River in the north. The water in the canal shows a salinity range from 0.46 to 21.96 g l^{-1} as shown in the graph of Fig. 5b. The maximum salinity was recorded at the end of the each monsoon period during this study. This was due to the mixing of seawater into the backwater at the end of each monsoon that will increase the concentration of salt in the canal. This canal was originally established for navigation, but now, it is used to collect storm water to moderate flood in south Chennai during monsoon (Shanmugam and Ambujam 2012). The increase of salinity may also due to the presence of salt in the topsoil and unsaturated zone by means of evaporates and sea spray that will be washed out into the canal by means of storm water.

The vertical two-dimensional profiles represent salinity variation within the aquifer (Fig. 6). The shape of the freshwater lens and its thickness follow the topographic relief, concentration gradient, and the groundwater level. The thickness of the freshwater lens is larger in the southern part (profile C-C′) than in the northern part (profile A-A′). The maximum thickness of freshwater (salinity < 1 g l^{-1}) is measured in the southern part (profile C-C′) of the study area and it is 13.7 m. The minimum thickness of the freshwater is measured in the northern part (profile A-A′) of the study area is 6.3 m. The thickness of freshwater in the middle part (profile B-B′) of the study area is 11.1 m. By comparing the thickness of freshwater measured from all the locations, it is apparent that the thickness of freshwater is less in the northern part of the area. In the partially isolated or elongated aquifer, high hydraulic conductivity generally shows a shallow interface between freshwater and seawater, whereas if the hydraulic conductivity is low, the interface is deeper. The northern part of the study area has smaller hydraulic conductivity than the remaining area to the south. The thickness of the freshwater lens in the profile A-A′ is smaller, and the interface is shallow than the other profiles. This is probably related to the fact that the quantity of groundwater pumping is larger in the northern part of the study area with respect to the southern part. The area close to the canal shows a higher salinity due to the presence of clay and influence of canal. By comparing the three profiles from south to north, a decreasing trend in the areal extent

Fig. 7 Migration of groundwater facies during the period of study
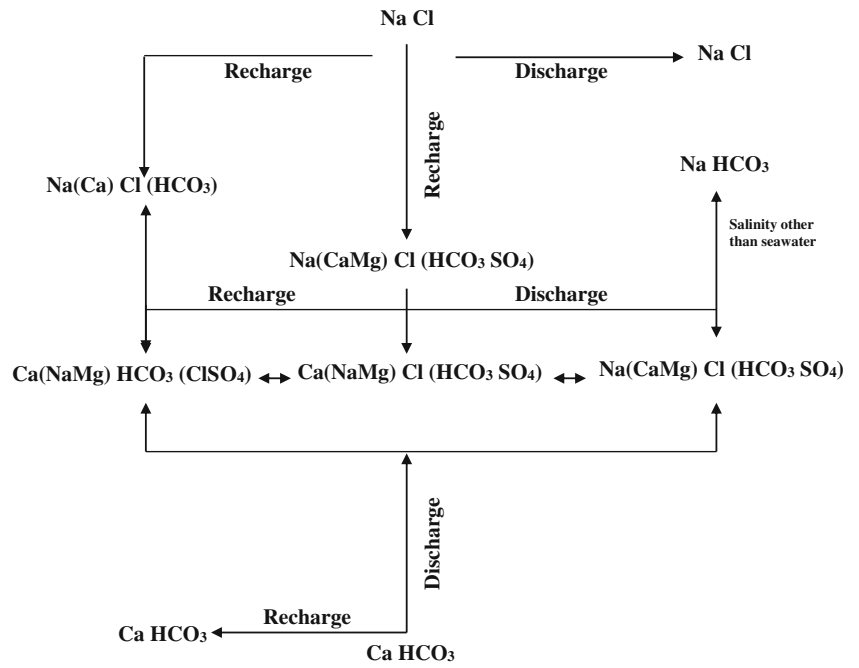
of freshwater lens is clearly observed. The freshwater lens in the profile A-A′ is mostly present towards westwards. The decrease in thickness and areal extent of the freshwater lens along the coastal boundary indicates the migration

of zone of seawater intrusion towards the landward side. VES survey carried out in the coastal zone of profile A-A′ also indicates a low apparent resistivity of 42.6 Ω-m, which confirms the seawater intrusion.

Fig. 8 a Piper diagram shows trend of salinization. **b** Comparison of groundwater level, rainfall, and BEX index
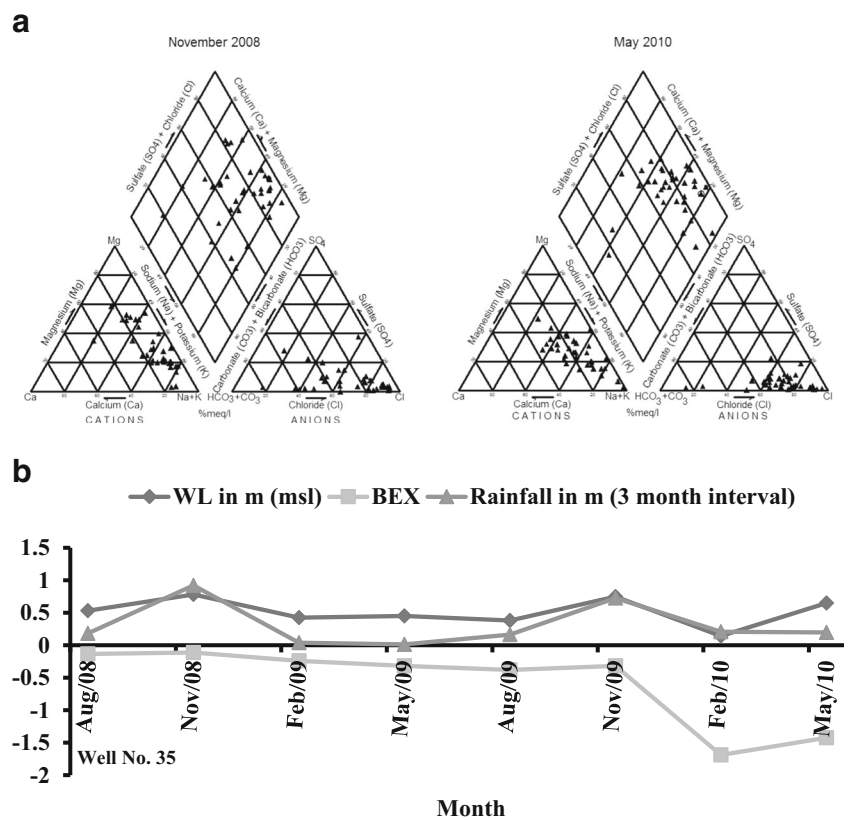
Table 3 BEX index calculated from the wells

Well no.	August 8	November 8	February 9	May 9	August 9	November 9	February 10	May 10
35	−0.1343	−0.1122	−0.2419	−0.3188	−0.3796	−0.3193	−1.6892	−1.4243
36	0.6895	0.4209	−0.1892	−0.2982	−0.3173	−0.2130	−0.0516	−0.9589
38	1.6162	1.7744	1.8332	1.6907	4.3170	5.2379	3.4661	0.8108
39	3.0576	2.1337	1.4029	2.7881	3.4154	3.3266	4.7663	2.1714
22	1.1939	1.1818	−2.7513	−0.5314	−0.2048	1.1143	0.6782	1.4816
23	2.0285	2.3382	1.7744	0.6393	−0.3888	−2.1205	1.5797	0.9598
24	−0.0406	2.3996	2.0953	0.6172	0.7433	1.3967	1.1320	1.1329
25	−0.2948	1.7239	−0.0797	−0.8363	0.7412	1.9014	1.0492	2.2194
26	1.8704	0.0317	4.6547	3.3119	0.5721	0.9507	6.2398	2.3171
12	0.2629	1.5359	0.4209	1.1150	0.9019	1.4565	1.8525	2.3606
11	0.1281	1.0118	0.8047	0.6246	0.5523	1.6073	1.4553	1.6910
Rainfall in mm (3-month interval)	181.5	920.6	37.2	12.5	163.7	726.6	206.0	195.0

Base exchange index

The classification of groundwater is used to a grouping of samples into particular type in the particular environmental zone. All among the water type classification methods, piper diagram is the point indicator of water type. In the current study, strong differences in the hydrogeochemical facies were noticed. The migration of groundwater facies during the period of study is given in Fig. 7. All the groundwater samples are representing the trend of freshening and salinization between the period of monsoon and dry season (Fig. 8a). The factors which control the hydrogeochemical facies of groundwater are lithology, groundwater flow pattern, and solution kinetics of the aquifer. The groundwater is dominated by Na^+-Cl^- type along the coastal boundary, and it is followed by Ca^{2+}-HCO_3^- towards inland. The location of the interface between freshwater and seawater and zone of mixing between them were controlled by the fluctuation of groundwater level which is controlled by the source of recharge and discharge from the aquifer. The BEX index calculation for coastal groundwater can give information about the trend of salinization and freshening of groundwater or into a state of conservative equilibrium between seawater and groundwater. The BEX index calculated from the hydrogeochemical data obtained from the wells was compared with groundwater levels, and rainfall is given in Fig. 8b. In general, the BEX index points out a salinization trend (BEX < 0) in the northern part of the study area due to the extensive residential settlements which cause over pumping and consequent seawater intrusion. The BEX index increase towards the south is indicating a better quality (freshening) of groundwater because of proper land use practice and least residential settlements. The northern part of the area close to the coastal zone (well nos. 35 and 36) is more saline due to the intrusion of seawater (Table 3). The negative BEX index is also observed in few locations other than these three profiles which point out an irregular pumping of groundwater depending upon the needs of individuals. In the western side, the monsoonal variation in salinization and freshening of the groundwater was not noticed due to the presence of clay that will slow the movement of groundwater. The salinity along the western boundary may due to the same reason that the clay will increase the residential time of groundwater. The salinity caused by agriculture activities is less compare to pumping of groundwater for domestic purposes. Even though in the southern part of the area occupied by cultivated land, the availability of thicker freshwater zone confirms that the influence of least agriculture activities.

Conclusion

The aquifer selected for the present study behaves as a partially isolated aquifer due to the presence of surface water on all the sides. The freshwater lens present in this aquifer is investigated by using electrical resistivity survey and hydrogeochemical analysis. The VES results identify the presence of four electrical resistivity layers in the western part bordering the canal and five electrical resistivity layers in the rest of the area that covers dune surface and coastal zone. The apparent resistivity values varying between 3.2 and 45.1 Ω-m indicate the influence of seawater which is noticed in all the locations investigated in the coastal zone except the locations C2 and C5. However, the seawater intrusion is significantly noticed in locations C-1 (north) and C-6 (south). These were correlated and confirmed with hydrogeochemical results. In the location C-1, a sudden decrease of apparent resistivity from several thousands to 42.6 Ω-m indicates seawater intrusion. The least value of 3.2 Ω-m noticed in the location C-6 also indicates the same.

The groundwater is dominated by Na^+-Cl^- type along the coastal boundary, and it is followed by Ca^{2+}-HCO_3^- towards inland. The presence of lower EC and elevated groundwater level in the middle of the each cross-sectional profile confirms the presence of the freshwater lens. Based on chloride concentration, the majority of the shallow groundwater samples are primarily of the oligohaline to fresh category in the dune surface and brackish to saline along the coastal zone. The change in the bicarbonate concentration also emphasizes the presence of freshwater in the south and quality degradation towards the north. The cross-sectional comparison of groundwater level and EC gives a better understanding of the influence of saltwater presence on all the sides. By comparing the three salinity profiles (A-A′, B-B′, and C-C′) from south to north, a decreasing trend in the areal extent of freshwater lens is clearly observed. From the salinity profile A-A′, it is clear that towards the northern part, the width of the aquifer is larger but the areal extent of the freshwater lens is smaller than the south. It indicates the heavy pumping of the groundwater that induced the intrusion of seawater and subsequent decrease in areal extent of the freshwater lens in the north. VES survey carried out in the coastal zone of profile A-A′ also indicates a low apparent resistivity of 42.6 Ω-m, which confirms the seawater intrusion. A comparative analysis of all the measured and calculated data shows that the interface between seawater and freshwater is migrating landward during the months of the dry period.

The comparison of BEX index with groundwater level and rainfall confirms the progressive trend of salinization in the northern part and freshening in the southern part. The BEX index also gives a clear idea that depicts a strong seasonality changes in salinity between monsoon and dry period. The negative BEX index is also observed in few locations in the wells located inland which point out an irregular pumping of groundwater. The wells located close to the canal does not represent significant monsoonal variations in the trend of salinization and freshening; however, the salinity is high due to the presence of clay. The present study clearly helps to understand the lateral and vertical variation of groundwater salinity and the process of salinization and freshening of groundwater under various seasons. From the present work, it is clear that the thickness of the freshwater lens and quality of groundwater is decreasing from south to north due to the extensive pumping to meet the needs. Hence, this study recommends that the pumping of groundwater in the northern part has to be reduced to recover the thickness and areal extent of freshwater lens and to maintain the natural hydrodynamics in this aquifer.

References

Adepelumi AA, Ako BD, Ajayi TR, Afolabi O, Omotoso EJ (2009) Delineation of saltwater intrusion into the freshwater aquifer of Lekki Peninsula, Lagos. Nigeria Environ Geol 56:927–933

Anderson WL (1989) A hybrid fast Hankel transform algorithm for electromagnetic modeling: geophysics. Soc Explor Geophys 54:263–266

Antonellini M, Mollema P, Giambastiani B, Bishop K, Caruso L, Minchio A, Pellegrini L, Sabi M, Ulazzi E, Gabbianelli G (2008) Salt water intrusion in the coastal aquifer of the southern Po Plain, Italy. Hydrogeol J 16:1541–1556

Apello CAJ, Willemsen A (1987) Geochemical calculations and observations on saltwater intrusions, a combined geochemical and mixing cell model. J Hydrol 94:313–330

Archie GE (1942) The electrical resistivity log as an aid in determining some reservoir characteristics. Trans AIME 146:54–62

Bakker M (2000) The size of the freshwater zone below an elongated island with filtration. Water Resour Res 36(1):109–117

Balkaya C, Ali Kaya M, Kaya MA (2009) Delineation of shallow resistivity structure in the city of Burdur, SW Turkey by vertical electrical sounding measurements. Environ Geol 57:571–581

Barker RD (1980) Application of geophysics in groundwater investigations. Water Surv 84:489–492

Bear J, Cheng AHD, Sorek S, Ouazar D, Herrera I (1999) Seawater intrusion in coastal aquifers—concepts, methods, and practices. Kluwer Academic Publishers, Dordrecht

Benkabbour B, Toto E, Fakir Y (2004) Using DC resistivity method to characterize the geometry and the salinity of the Plioquaternary consolidated coastal aquifer of the Mamora plain. Morocco Environ Geol 45:518–526

Bereslavskii EN (2006) Influence of the inclination of the sea floor (slope) on intrusion in littoral zones. J Eng Phys Thermophys 79(6):1193–1201

Bernard J (2003) Definition of main hydrogeological parameters. Electrical methods for groundwater. Magnetic resonance method for groundwater. Short note on the principles of geophysical methods for groundwater investigations

Corriols M, Dahlin T (2008) Geophysical characterization of the leon-chinandega aquifer. Hydrogeol J 16(2):355

Cox RA, Culkin F, Riley JP (1967) The electrical conductivity/chlorinity relationship in natural seawater. Deep-Sea Res 14:203–220

CRZ (2010) Proposed coastal regulation zone notification (2010), Ministry of Environment and Forest Report https://www.goa.gov.in/portalweb/com/infotech/…/predraftCRZ.pdf

Davis PA, Greenhalgh SA, Merrick NP (1980) Resistivity sounding computations with any array using a single digital filter. Bull Aust Soc Explor Geophys 11:54–62

De Franco R, Biella G, Tosi L, Teatini P, Lozej A, Chiozzotto B, Giada M, Rizzetto F, Claude C, Mayer A, Bassan V, Gasparetto-Stori G (2009) Monitoring the saltwater intrusion by time lapse electrical resistivity tomography: the Chioggia test site (Venice Lagoon, Italy). J Appl Geophys 69:117–130

Delecourt J (1941) Le Titre natronique (1re note). Bull Soc belge de Geol Paleont et Hydrol 50:152–166

Elango L, Ramachandran S, Chowdary YSN (1992) Groundwater quality in coastal regions of south Madras. Indian J Environ Health 34(4): 318–325

Fetter (2001) Applied hydrology, 4th edn. Prentice-Hall, Inc, Upper Saddle River, p 367

Garman KM, Purcell SF (2004) Three-dimensional electrical resistivity surveys to identify buried karst features affecting road projects. Subsurface Evaluations, Inc., Woodland Center Blvd., Tampa, Fl 33614

Gimenez Forada E (2010) Dynamic of sea water interface using hydrochemical facies evolution diagram. Groundwater 48(2):212–216

Gnanasundar D, Elango L (1998) Groundwater quality of a coastal urban aquifer. Indian J Environ Prot 18(10):752–757

Gnanasundar D, Elango L (1999) Groundwater quality assessment of a coastal aquifer using geoelectrical techniques. Int J Environ Hydrol 7(2):21–33

Gnanasundar D, Elango L (2000) Groundwater flow modeling of a coastal aquifer near Chennai city, India. J Indian Water Res Soc 20(4): 162–171

Griffiths DH, Barker RD (1993) Two-dimensional resistivity, imaging and modeling in areas of complex geology. J Appl Geophysics 29(3-4):211–226

Goldman M, Gilad D, Rouen A, Melloul A (1991) Mapping of seawater intrusion into the coastal aquifer of Israel by the time domain electromagnetic method. Geoexploration 28:153–174

Gondwe E (1990) Saline water intrusion in southeast Tanzania. Geoexploration 27(199):25–34

Hinrichsen D (2007) Ocean planet in decline. http://www.peopleandplanet.net/?lid=26188&topic=44&section=35. Accessed 1 Jun 2011

Hodlur GK, Dhakate R, Sirisha T, Panaskar DB (2010) Resolution of freshwater and saline water aquifers by composite geophysical data analysis methods. Hydrol Sci J 55(3):414–434

Inman JR (1975) Resistivity inversion with ridge regression. Geophysics 40(5):798–817

IPCC (2007) IPCC, 2007: climate change 2007: impacts, adaptation and vulnerability. Contribution of Working Group II to the Fourth Assessment Report of the Intergovernmental Panel on Climate Change

Jupp DLB, Vozoff K (1975) Stable iterative methods of inversion of geophysical data. Geophys J Int 42(3):957–976

Keller G, Frischknecht F (1966) Electrical methods in geophysical prospection. In: International series in electromagnetic waves, Vol. 10, Pergamon Press, Oxford

Kelly WE (1977) Geoelectric sounding for estimating aquifer hydraulic conductivity. Groundwater 15(6):420–425

Knudsen M (1901) Hydrographical tables according to the measuring of Carl Forch, P. Jacobsed, Martin Knudsen and S.P.L. Sorensen, G.E.C. Gad: Copenhagen: Williams Norgate, London, pp. 63

Kooi H, Groen J, Leijnse A (2000) Modes of seawater intrusion during transgressions. Water Resour Res 36(12):3581–3589

Kouzana L, Benassi R, Mammou AB, Felfoul SM (2010) Geophysical and hydrochemical study of the seawater intrusion in mediterranean semi arid zones, case of the Korba coastal aquifer (Cap-Bon, Tunisia). J Afr Earth Sci 58(2):242–254

Kuzhali M, Ambujam NK, Karunakaran K (2009) Blue gold conservation—the road to sustainability. In proc. World Water Week, Stockholm, 16-22 August 2009

Lee JY, Song SH (2006) Evaluation of groundwater quality in coastal areas: implications for sustainable agriculture. Environ Geol 52: 1231–1242

Lee JY, Song SH (2007) Evaluation of groundwater quality in coastal areas: implications for sustainable agriculture. Environ Geol 52: 1231–1242

Massoud U, Soliman M, Taha A, Khozym A, Salah H (2015) 1D and 3D inversion of VES data to outline a freshwater zone floating over saline water body at the northwestern coast of Egypt. NRIAG J Astron Geophys 4(2):283–292

Mollema PN, Antonellini M, Dentinho T, Silva VRM (2010) The effects of climate change on the hydrology of groundwater of Terceira island (Azores). Proc. 21st Salt Water Intrusion Meeting, Azores, Portugal, 21-26 June 2010

Mondal NC, Singh VS, Saxena VK, Singh VP (2011) Assesment of seawater impact using major hydrochemical ions: a case study from Sadras, Tamilnadu, India. Environ Monit Asses 177:315–335

Nowroozi AA, Stephen BH, Henderson P (1999) Salt water intrusion into the freshwater aquifer in the eastern shore of Virginia: a reconnaissance electrical resistivity survey. J Appl Geophys 42:1–22

Oskay MM, Orcan OA, Kissami M (1993) Determination of formation resistivity factors using step increases of temperature. J Pet Sci Eng 8:333–335

Oude Essink GHB (2001) Improving fresh groundwater supply—problems and solutions. Ocean Coast Manag 44:429–449

Park YH, Doh SJ, Yun ST (2007) Geoelectric resistivity sounding of riverside alluvial aquifer in an agricultural area at Buyeo, Geum River watershed, Korea: an application to groundwater contamination study. Environ Geol 53:849–859

Post VEA, Simmons CT (2005) Free convective controls on sequestration of salts into low-permeability strata: insights from sand tank laboratory experiments and numerical modeling. Hydrogeol J 18:39–54

Sathish S, Elango L (2011) Groundwater quality and vulnerability mapping of an unconfined coastal aquifer. J Spat Hydrol 11:18–33

Sathish S, Elango L (2015) Numerical simulation and prediction of groundwater flow in a coastal aquifer of Southern India. J Water Res Prot 7:1483–1494

Sathish S, Elango L, Rajesh R, Sarma VS (2011) Assessment of seawater mixing in a coastal aquifer by high resolution electrical resistivity tomography. Int J Environ Sci Tech 8(3):483–492

Schlumberger C (1920) Study of underground electrical prospecting. Gaultier-Villars et Cie., Paris. https://archive.org/stream/studyofundergrou00schlrich#page/n7/mode/2up.

Schoeller H (1934) Les échanges de bases dans les eaux souterraines; trois exemples en Tunisie. Bull Soc Geol Fr 4:389–420

Schoeller H (1956) Geochemie des eaux souterraines. Revue de l'Instit Francaise du Petrole 10:230–244

Senthil Kumar M, Gnanasundar D, Elango L (2001) Geophysical studies to determine hydraulic characteristics of an alluvial aquifer. J Environ Hydrol 9(15):1–8

Shanmugam P, Ambujam NK (2012) A hydrochemical and geological investigation on the Mambakkam mini watershed, Kancheepuram District, Tamil Nadu. Environ Monit Assess 184:3293–3306

Shevnin V, Rodriguez OD, Mousatov A, Hernandez DF, Martinez HZ, Ryjov A (2006) Estimation of soil petrophysical parameters from resistivity data: application to oil-contaminated site characterization. Geofisica Internacional 45(3):179–193

Shevnin V, Mousatov A, Ryjov A, Rodriguez V (2007) Estimation of clay content in soil based on resistivity modelling and laboratory measurements. Geophys Prospect 55:265–275

Sivakumar C, Elango L (2010) Application of solute transport modeling to study tsunami induced aquifer salinity in India. J Environ Inform 15(1):33–41

Smith D, Johnson CC (2011) Distribution of iodine in soils of northern Ireland. Geochem: Explor Environ Anal 11(1):25–39

Sonkamble S (2014) Electrical resistivity and hydrochemical indicators distinguishing chemical characteristics of subsurface pollution at Cuddalore Coast, Tamil Nadu. J Geophys Soc India 83:535–548

Srinivasa Gowd SS (2004) Electrical resistivity surveys to delineate groundwater potential aquifers in Peddavanka watershed, Anantapur District, Andhra Pradesh, India. Environ Geol 46:118–131

Stollar RL, Roux P (1975) Earth resistivity survey—a method for defining ground-water contamination. Groundwater 13(2):145–150

Stuyfzand PJ (1986) A new hydrochemical classification of water types: principles and application to the coastal dunes aquifer system of the Netherlands. Proc. 9th Salt Water Intrusion Meeting, Delft, The Netherlands, 12-16 May 1986

Stuyfzand PJ (1993) Hydrochemistry and hydrology of the coastal dune area of the Western Netherlands. Ph.D. thesis, Vrije Universiteit Amsterdam, The Netherlands, pp. 366

Stuyfzand PJ (2008) Base exchange indices as indicators of salinization or freshening of (coastal) aquifers. In proc. 20th Salt Water Intrusion Meeting, Naples, Florida, USA, 23-27 June 2008

Sundberg K (1932) Effect of impregnating waters on electrical conductivity of soils and rocks. Trans AIME 97:367–391

UNESCO (1981a) Background papers and supporting data on the practical salinity scale, 1978. UNESCO Tech. Pap. Mar. Sci., 38, pp. 192

UNESCO (1983) Algorithms for computation of fundamental properties of seawater, 1983. UNESCO Tech Pap Mar Sci 44:6–9

Vengosh A (2003) Salinization and saline environment. Treatise Geochem 9:333–365

Versluys J (1916) Chemische werkingen in den ondergrond der duinen. Verslag Gewone Vergad. Wis & Nat afd Kon Acad Wetensch Amsterdam 24:1671–1676

Versluys J (1931) Subterranean water conditions in the coastal regions of The Netherlands. Econ Geo 26:65–95

Waxman MH, Smith LJM (1968) Electrical conductivities in oil bearing sands. J Soc Pet Eng 8:107–122

Worthington PF (1993) The uses and abuses of the Archie equations, 1: the formation factor-porosity relationship. J Appl Geophys 30:215–228

Yadav GS, Singh SK (2007) Integrated resistivity surveys for delineation of fractures for groundwater exploration in hard rock areas. J Appl Geophys 62:301–312

Zhang J, Huang WW, Letolle R, Jusserand C (1995) Major element chemistry of the Huanghe (Yellow River), China weathering processes and chemical fluxes. J Hydrol 168(94):173–203